ADVANCED TECHNOLOGY CENTER, INC.

N73-15723

FINAL REPORT

MEASUREMENTS OF ELECTRON-BREMSSTRAHLUNG COINCIDENCE RATES AT INTERMEDIATE ELECTRON ENERGIES

Report No. B-94200/2CR-55

October 1972

The Research Center of LTV Aerospace Corporation and LTV Electrosystems, Inc.

N73-15723

N73-15723

FINAL REPORT

MEASUREMENTS OF ELECTRON-BREMSSTRAHLUNG COINCIDENCE RATES AT INTERMEDIATE ELECTRON ENERGIES

Report No. B-94200/2CR-55

October 1972

FINAL REPORT

CONTRACT NO. NAS8-27866

Period Covering November 1, 1971 through November 1, 1972

MEASUREMENTS OF ELECTRON-BREMSSTRAHLUNG COINCIDENCE RATES AT INTERMEDIATE ELECTRON ENERGIES

by

D. H. Rester

ATC Report No. B-94200/2CR-55

October 1972

Prepared for

GEORGE C. MARSHALL SPACE FLIGHT CENTER

NATIONAL AERONAUTICS AND SPACE ADMINISTRATION

HUNTSVILLE, ALABAMA

Prepared by

ADVANCED TECHNOLOGY CENTER, INC.

DALLAS, TEXAS 75222

TABLE OF CONTENTS

ABSTRACT

Coincidence rates have been measured for inelastically scattered electrons and their associated bremsstrahlung for bombarding energies of 0.20 and 0.15 MeV. Measurements were made for an electron angle of 45 deg and a photon angle of 20 deg. Inelastic electron energies of 0.15 and 0.16 MeV were considered for an incident energy of 0.2 MeV and an inelastic electron energy of 0.12 MeV was considered for an incident energy of 0.15 MeV. To observe the trend with atomic number, Al and Au targets were used. The experimental cross sections differential in photon and electron angles and energy were found to be smaller than the predictions of the Bethe-Heitler theory.

MEASUREMENTS OF ELECTRON-BREMSSTRAHLUNG COINCIDENCE RATES AT INTERMEDIATE ELECTRON ENERGIES

INTRODUCTION

The coincidence rates for the detection of inelastically scattered electrons and the associated photons, or bremsstrahlung, have been measured for two bombarding energies, 0.20 and 0.15 MeV. Cross section values differential in photon angle, electron angle, and energy for Al and Au targets have been calculated from the experimentally determined coincidence rates for a photon angle of 20 deg and an electron angle of 45 deg.

The determination of inelastic electron-photon coincidence rates is the culmination of a series of measurements describing the interactions of electrons of intermediate energy with atomic scattering centers. Earlier experiments[1-11] were completed leading to the determination of bremsstrahlung cross sections uncorrelated with the scattered electrons, electron elastic scattering cross sections, and electron inelastic scattering cross sections uncorrelated with photons for incident electron energies from 0.05 to 2.5 MeV. Target materials representative of a wide range of atomic number, from Be ($Z = 4$) to Au ($Z = 79$), were used.

In the early stages of the electron interactions program emphasis was placed on experimentally defining an extensive set of accurate bremsstrahlung cross section values. It was the early objective of the program to provide these for use in a multiple scattering, Monte Carlo computer program being developed at the National Bureau of Standards. The measured bremsstrahlung cross sections were incorporated in the multiple scattering program, and comparisons[7,9] of calculated spectra from the Monte Carlo program with experimental thick target spectra verified the accuracy of the computational technique. Subsequent work in which there was more detailed inputting of the experimental cross section values to the computer code indicated that even for high-Z materials at low bombarding energy agreement was observed between the experimental and calculated spectra.

The next phase of the electron interaction studies has been the measurement of electron inelastic scattering cross sections and electron-bremsstrahlung

coincidence rates. The objective of these measurements is to provide data for comparison to theoretical cross section values which appeared to be forthcoming from the work of Brysk, Zerby, and Penny.[12] Recent comparisons[6,11] of bremsstrahlung cross section values from their work with experimental values, however, revealed deficiencies in the theoretical effort which are most likely due to the complexity of the computer program written to evaluate the formulas. It is clearly difficult to evaluate cross sections accurately by use of the existing Zerby-Brysk-Penny Code at bombarding energies above 200 keV. It has been found that even below 200 keV inadequacies in the calculations exist for some photon energy regions for low-Z targets. Nevertheless limited experimental values of the inelastic electron scattering cross sections and the electron-bremsstrahlung doubly differential cross section have been obtained for comparison to theoretical values beyond the Born-approximation when they are computed.

The coincidence measurements from which five cross section values have been reduced are described in this report. No previous study has been found in which measurements of absolute inelastic electron-bremsstrahlung coincidence yields are reported. Targets of Al and Au were used in the measurements to observe the effect of atomic number on the cross section values. The choice of electron scattering angle and photon angle was limited, however.. The angular correlation curves from the Born-approximation theory, which is believed to predict the position of the maximum yield accurately, if not the magnitude of the cross sections, indicates that the highest coincidence rate for a fixed electron angle other than zero occurs for a photon angle in the scattering plane on the same side of zero (at smaller angle) as the electron angle. With the rather large detection apparatus employed in the experiment, a magnetic analyzer and a low temperature Ge(Li) photon spectrometer, it was not possible to make the measurement for an electron scattering angle less than about 45 deg. For an electron angle of 45 deg the predicted maximum in the angular correlation curve occurs at a photon angle of 20 deg. A considerable effort was made initially to ensure that the results of independent measurements in the electron and the photon channels in the coincidence geometry were consistent with the corresponding measurements in what was considered to be the best geometries for the individual measurements.

The measurement of the inelastically scattered electron spectra for a bombarding energy of 0.2 MeV (in which all interactions leading to inelastic events were observed) indicated that the yield in the energy region of the coincidence measurement exceeded the Bethe-Heitler estimate. However the broadening of the electron-electron line and its shape on the high energy side led to the conclusion that a large contribution to the inelastic yield at higher energies must arise from electron-electron scattering. The presently reported measurements confirm this conclusion, since the coincidence technique eliminates all inelastic events except the radiative events and yields less than the Bethe-Heitler predictions were obtained.

EXPERIMENTAL METHOD

A diagram of the experimental geometry is shown in Fig. 1. A mono-energetic electron beam was provided by the Cockcroft-Walton electron accelerator. The beam was steered to a cylindrical scattering chamber and focussed at the center (target position) so that the spot size, as observed on a ZnS fluorescent screen, was about 1 mm in diameter. The focal length of the electro-static lens used to focus the parallel beam emerging from the accelerator was long enough that negligible error resulted from the finite electron convergence angle. A magnetic analyzer was positioned at the scattering angle of 45 deg. High resolution detection of the electrons accepted by the magnetic analyzer was actually achieved by use of a Si electron spectrometer at the focal position of the analyzer. Provision was made to cool the detector to improve its resolution if necessary. However for the measurements reported, the resolution of 12-16 keV normally obtainable with the spectrometer at room temperature was adequate. The photon spectrometer consisted of a planar-type Ge(Li) crystal detector and pre-amplifier system mounted on a cold-finger. The Ge crystal and first stage of the pre-amplifier were operated at liquid nitrogen temperature with a resolution of about 1 keV. A Ge(Li) spectrometer of this type is sensitive to x rays down to a few keV and has an efficiency of almost 100% in the photon energy region of interest here, i.e. 25 to 55 keV.

The function of the magnetic analyzer shown in Fig. 1 was to remove the very intense yield of elastically scattered electrons, which would otherwise saturate the detector at reasonable beam currents. By removing the elastic electrons it was possible to detect the inelastic electron group potentially in coincidence with the bremsstrahlung spectrum almost free from background interference. This is illustrated by the electron spectra shown in Figs. 2-3. In Fig. 2 spectra of magnetically analyzed electrons are plotted for magnetic field intensities corresponding to 0.16 and 0.15 MeV. A bombarding energy of 0.2 MeV was used for an Al target. Prominent, well resolved inelastic electron lines at 0.16 and 0.15 MeV were obtained. A line in each case at the incident energy of 0.2 MeV from the elastic scattering is also seen because of the finite resolving power of the magnet. However the intensities of the elastic peaks were reduced by several orders of magnitude. In

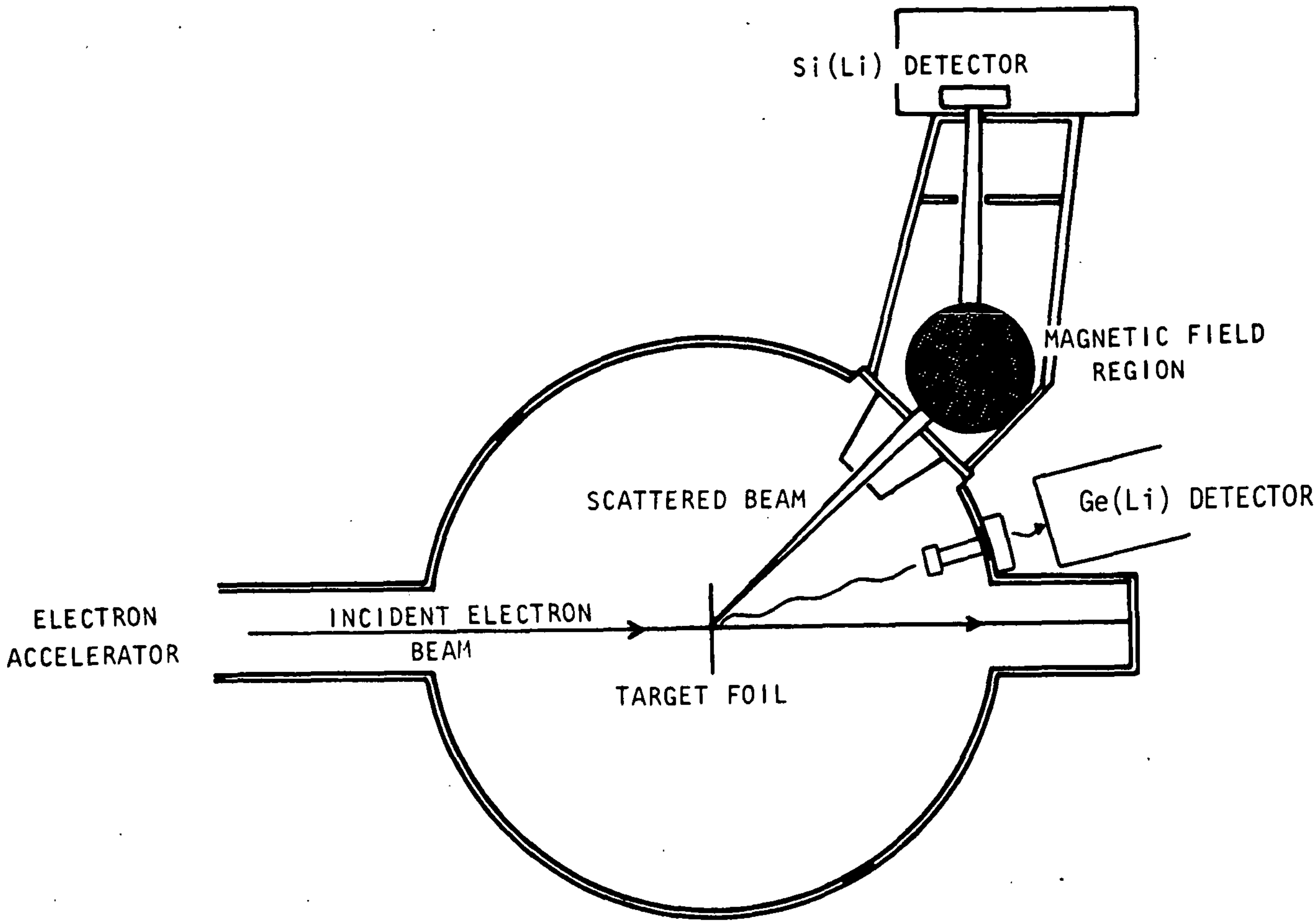

Fig. 1 Diagram of experimental geometry for coincidence rate measurements. The scattered electron beam was magnetically analyzed and detected by a high resolution spectrometer. A scattering angle of 45 deg was used. Target bremsstrahlung emitted at 20 deg was detected by a Ge(Li) spectrometer.

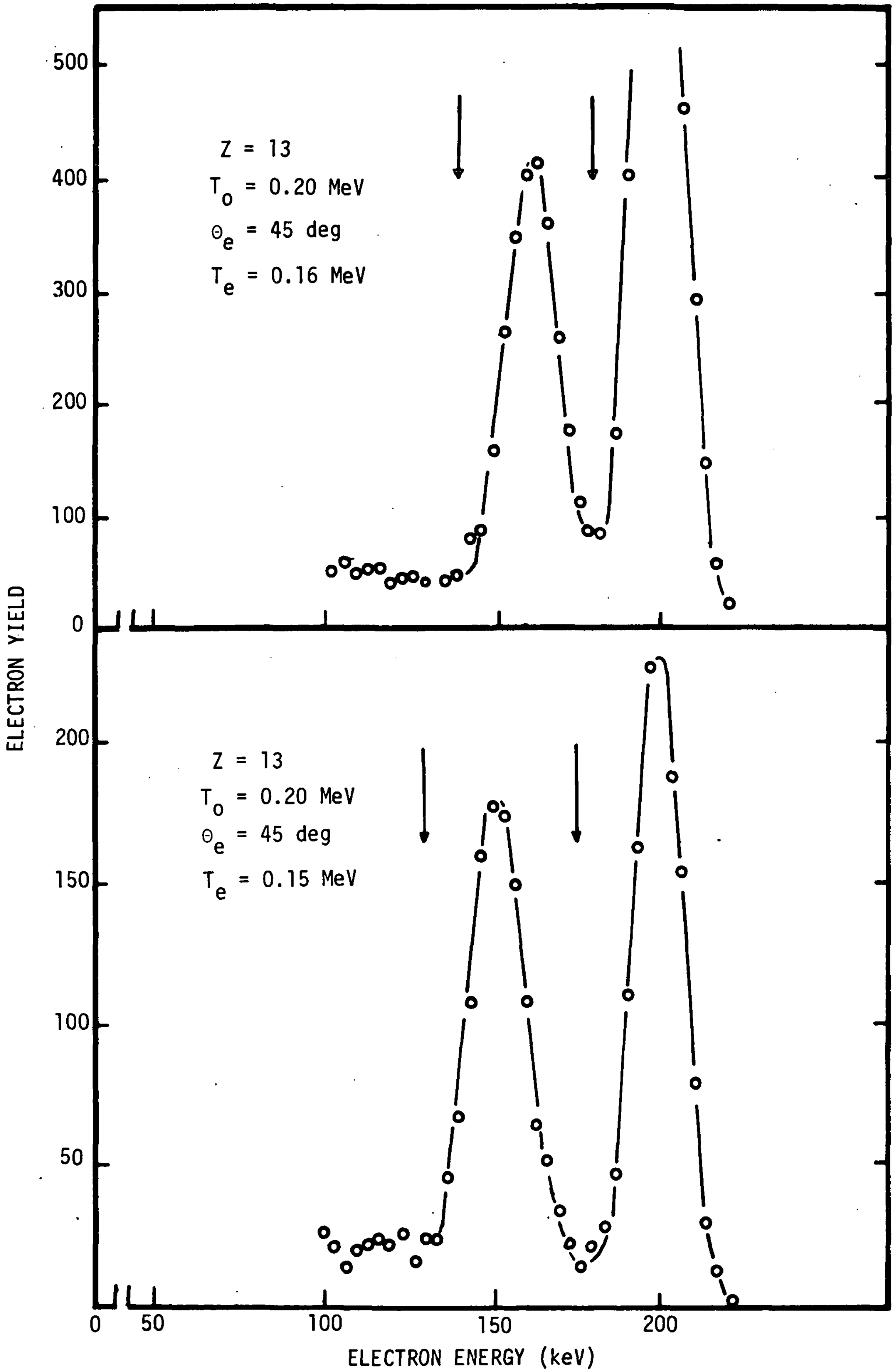

Fig. 2 Spectra of electrons measured by the electron spectrometer for magnetic analyzer settings corresponding to 0.16 and 0.15 MeV.

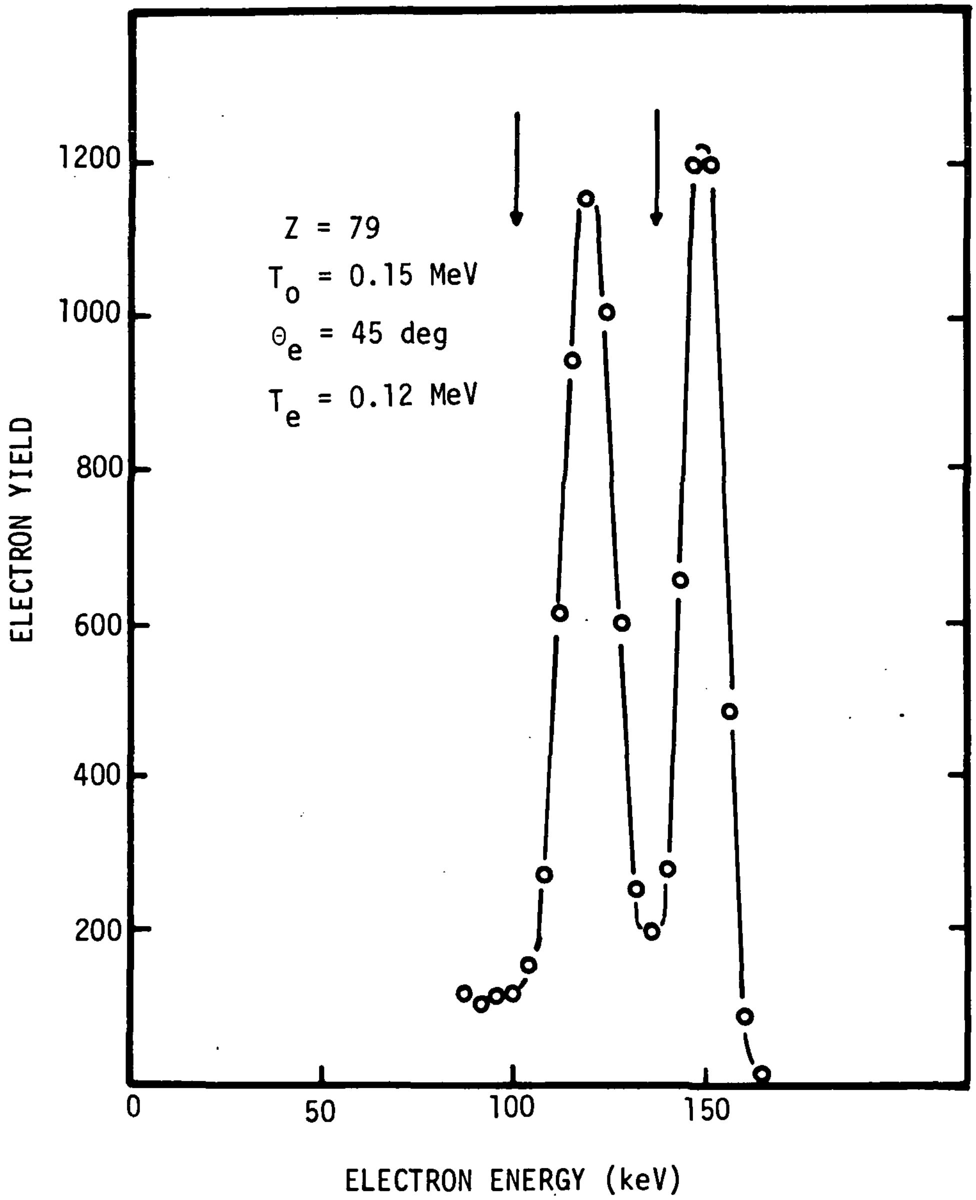

Fig. 3 Spectrum of electrons measured by the electron spectrometer for a magnetic analyzer setting corresponding to 0.12 MeV and for a bombarding energy of 0.15 MeV.

the coincidence counting mode a pulse height window corresponding to an electron energy increment was electronically set as indicated by the vertical arrows in the figure. Thereby the pulses from all regions of the spectra except those which were possible components of coincidence events, as determined by the kinematics of the interaction, were eliminated. Without deflection of the very intense elastic line from the exposed Si(Li) detector, the inelastic electron group of interest would have been submerged in the tail of the detector response to the elastics. At an incident energy of 0.2 MeV the inelastic electron yield in the electron energy region from 120-180 keV is approximately an order of magnitude less than that due to the response to the elastic line in the same region.

The spectrum of Fig. 3 is for a bombarding energy of 0.15 MeV. The magnetic analyzer was set to accept scattered electrons of 0.12 MeV. Somewhat higher energy resolution was used for the 0.15-MeV experiment, because the separation of the two lines as shown in the figure was only 30 keV. The improvement in energy resolution was achieved by using different time constants in the main amplifier of the electron channel. Some degradation of the time resolution resulted, but the increase in coincidence yield for the experiment at 0.15 MeV more than offset the increase in the accidental coincidence rate from poorer time resolution.

The port in the chamber wall through which photons were detected after collimation was vacuum sealed by a 10-mil thick Al window. This window, together with the vacuum window of the Ge spectrometer, was adequate to prevent scattered electrons of energies up to 0.2 MeV from reaching the Ge crystal. Attenuation of the photon flux in the Al window material was determined experimentally by interposing an additional 10-mil thickness of Al between the chamber and the spectrometer. Measurements of a continuous thick target bremsstrahlung spectrum were made with and without the additional material in place to obtain a correction curve as a function of photon energy. A 25% correction was necessary at a photon energy of 25 keV, the lowest energy considered in the coincidence measurements.

Background in the photon channel resulting from stopping the electron beam in the Faraday cage immediately adjacent to the Ge spectrometer was effectively eliminated by shielding the detector crystal. Photon spectra measured

in the coincidence geometry are shown in Figs. 4-5 for both Al and Au targets. Also shown, as solid circles, are the spectra obtained in a good geometry experiment for which it was possible to remove the background accurately. The energy increments corresponding to the inelastic electron lines of Fig. 2 are indicated in the figures. In the photon energy increments considered in the coincidence measurements a residual background yield of about 10-15% is apparent. A background of this magnitude had an insignificant effect on the accidental coincidence rate. A comparison of measurements with the spectrometer viewing the target and with the target blanked out by a Pb cylinder were also made to verify that only 15% of the total counts detected were due to background sources. Significant attenuation in the chamber window is seen in Figs. 4-5 at energies below 30 keV, where the singles spectra cross the experimental curves from the good geometry measurements.

The target foils used in the experiment were fabricated by standard vacuum evaporation techniques. Aluminum targets were made by evaporation onto a water soluble substrate and were subsequently floated off as self-supporting target foils. Target thicknesses for the case of Al were typically in the range from 20-50 $\mu g/cm^2$. It was not possible to make self-supporting targets of Au of the thicknesses required for the present measurements. Instead Au was evaporated onto 20-$\mu g/cm^2$ VYNS backings. Typically 50-70 $\mu g/cm^2$ of Au were used.

The coincidence technique used in the measurements provided multichannel pulse height analysis of the photon spectrum when selected conditions of time coincidence and energy span were met in the two channels. Single channel analyzers following the amplifier units in both channels placed energy limits on the radiations processed by the following stages of the coincidence system. The limits in the electron channel coincided with the windows shown in Figs. 2-3. Slightly wider limits were used in the photon channel than the 10-keV increments shown in Figs. 4-5, since the actual effective window considered was determined after pulse height analysis of events satisfying the time requirements. The use of slightly wider limits was desirable because of the uncertainties in the energy calibrations and the possibility of electronic instability during data accumulation periods, which often were up to ten hours in duration.

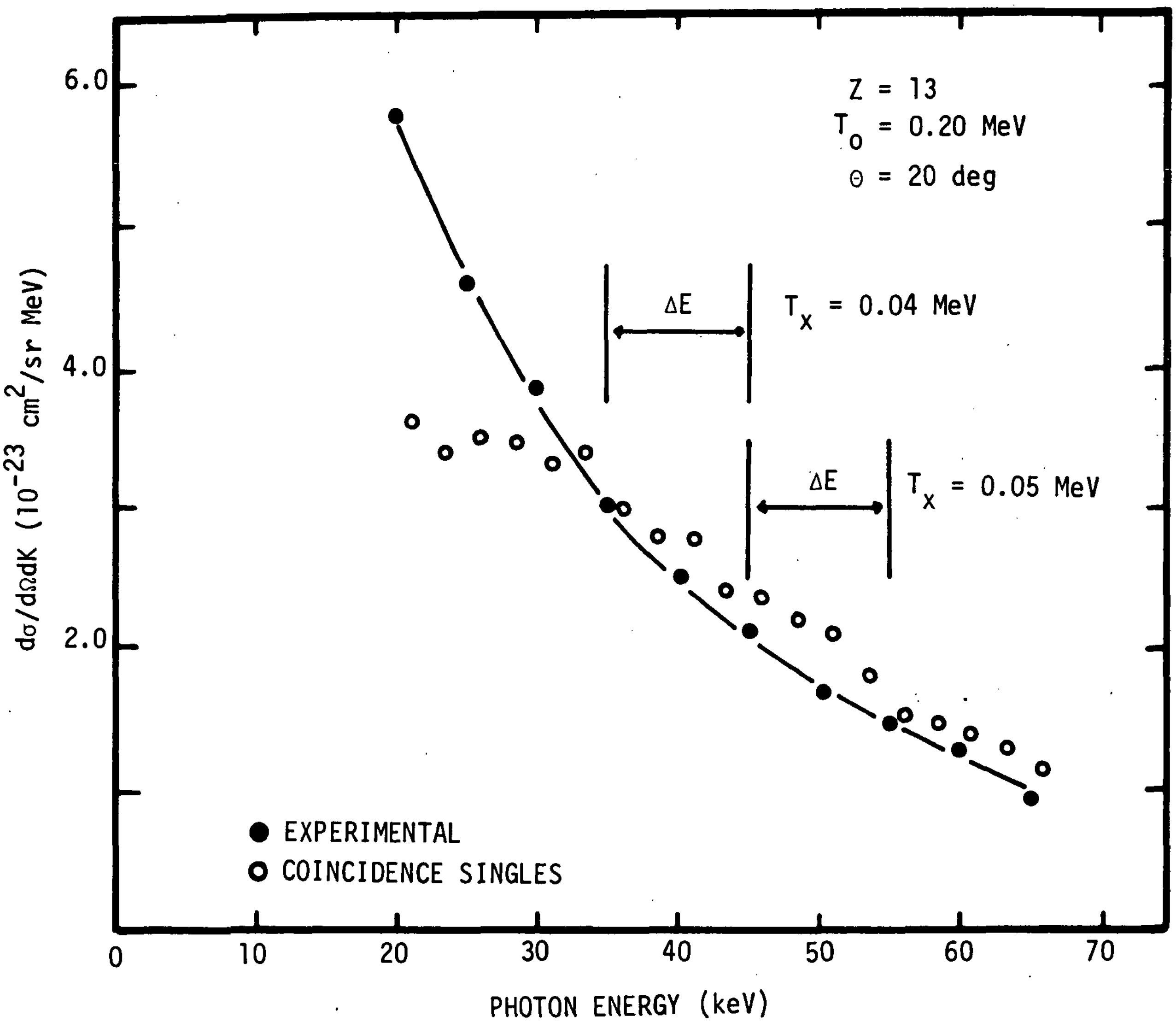

Fig. 4 Bremsstrahlung spectrum measured for Al in the coincidence geometry compared with spectrum measured in an ideal geometry with background removed.

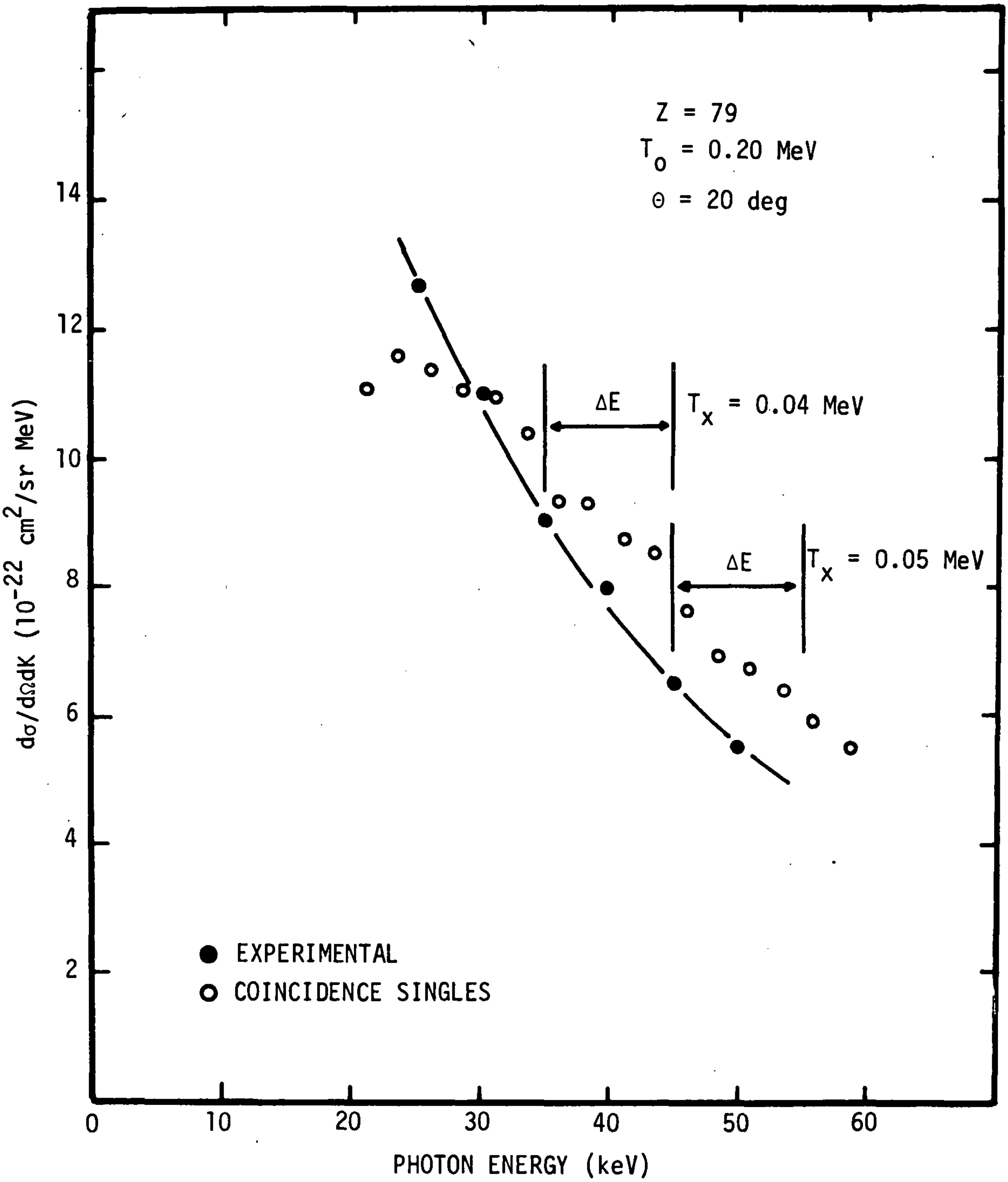

Fig. 5 Bremsstrahlung spectrum measured for Au in the coincidence geometry compared with spectrum measured in an ideal geometry with background removed.

Pulse-shaping of pulses from the pre-amplifiers was accomplished by the use of amplifiers with either RC pulse shaping networks (with selectable time constants) or delay line pulse differentiation. For the best possible timing of detected events with amplified pulses, double differentiated, bipolar pulses were used. The bipolar output pulses were processed by single channel analyzers. If the energy requirements were satisfied, output logic pulses were generated at the time of baseline crossover of the bipolar pulses. A variable delay of 0-100 μsec was provided in each channel between the generation of the logic pulses and the processing of the pulses by a fast coincidence system. The output logic pulses from the two single channel analyzers then were examined for time coincidence by the fast coincidence system.

The fast coincidence system provided for variable time resolution ranging from 10-110 nanosec. Selection of the resolving time actually used in the experiment was made after measurements of the inherent time spread of the two channels. These measurements also allowed the variable time delays in the channels preceding the time analysis to be adjusted so that true coincidence events would fall within the range of the coincidence network. Simultaneous radiations from a Hg^{203} source provided a high coincidence rate so that adjustments could be made in a relatively short period. Internal conversion electrons from the K shell of radioactive atoms were detected in coincidence with the fluorescence K x rays. The K-shell electron energy for the Hg^{203} transition energy of 279 keV is 194 keV and the prominent K x ray lines have energies of 71 and 73 keV. The energy differences of the radiations from the source and those observed in the case of the accelerator-produced radiations resulted in less than a 5-nanosec shift in the time correlation between the channels. This shift arose primarily from the differences in the penetration depths of the electrons in the detector materials, with a resulting variation in the charge collection times of the detector ionization which produces the output pulses. By use of a time to pulse height converter in place of the fast coincidence system a time spectrum of the coincidence events from the source was obtained. An inherent time spread of 50 nanosec was observed. A time resolution of 80 nanosec, therefore, allowed essentially all the true coincidence events to be counted and was used in the experiment. A reduction in the time window could have been made to improve the signal to background

ratio if the accidental coincidence rate had proven to be significant relative to the true rate.

The output logic pulse from the coincidence system, produced when input pulses were received within a time window of 80 nanosec, were routed to a linear gate. Unipolar analog pulses from the amplifier in the photon channel were also routed to the linear gate. Analog pulses were pulse height analyzed if the linear gate simultaneously received output pulses from the coincidence system. From the pulse height spectrum a bremsstrahlung spectrum in coincidence with inelastically scattered electrons was obtained.

DISCUSSION OF RESULTS

Before the coincidence work could be done it was necessary to measure the bremsstrahlung spectra for Al and Au for an incident energy of 0.2 MeV. A previous measurement had been made with a NaI crystal scintillation detector, but the rapidly changing response of NaI in the low energy region due to the iodine escape peak made the accuracy of the measurement in the low photon energy region questionable. Furthermore, a re-measurement of the spectra with the Ge(Li) spectrometer with high resolution was desirable in itself. Because of the importance of low energy data for comparison to theoretical values not only were Al and Au targets used but also a Cu target, so that the Coulomb effect and screening could be systematically observed as a function of atomic number. The results[11] of these measurements were published and the results for Al and Au are shown in Figs. 6-9.

The total inelastic electron spectra at 0.2 MeV incident energy had been previously measured in the geometry used for the coincidence measurements. The inelastic electron spectra are shown in Figs. 10-11. The portion of the inelastic electron energy distributions considered in the coincidence work is the region at energies greater than the electron-electron line at 93 keV. The contribution to the spectrum of electrons of energies greater than 100 keV from electron-electron interactions, where primarily bremsstrahlung-scattered electrons are expected to be observed, can not be determined from the singles spectra alone.

Two coincidence measurements were made for Al and Au targets at a bombarding energy of 0.2 MeV to obtain a better understanding of the relative contributions of various interactions leading to inelastic scattering. Inelastic electrons of energies of 0.15 and 0.16 MeV (photon energies of 0.05 and 0.04 MeV) were detected in coincidence with their associated bremsstrahlung. In addition, a single measurement on Au was made for an incident energy of 0.15 MeV and an inelastic electron energy of 0.12 MeV. Since the cross sections for the events as singles had been accurately determined, good estimates of the optimum electron beam currents and solid angle factors were made by computing the expected coincidence yields from the Bethe-Heitler theoretical values. At the same time it was possible to limit the accidental coincidence rates to

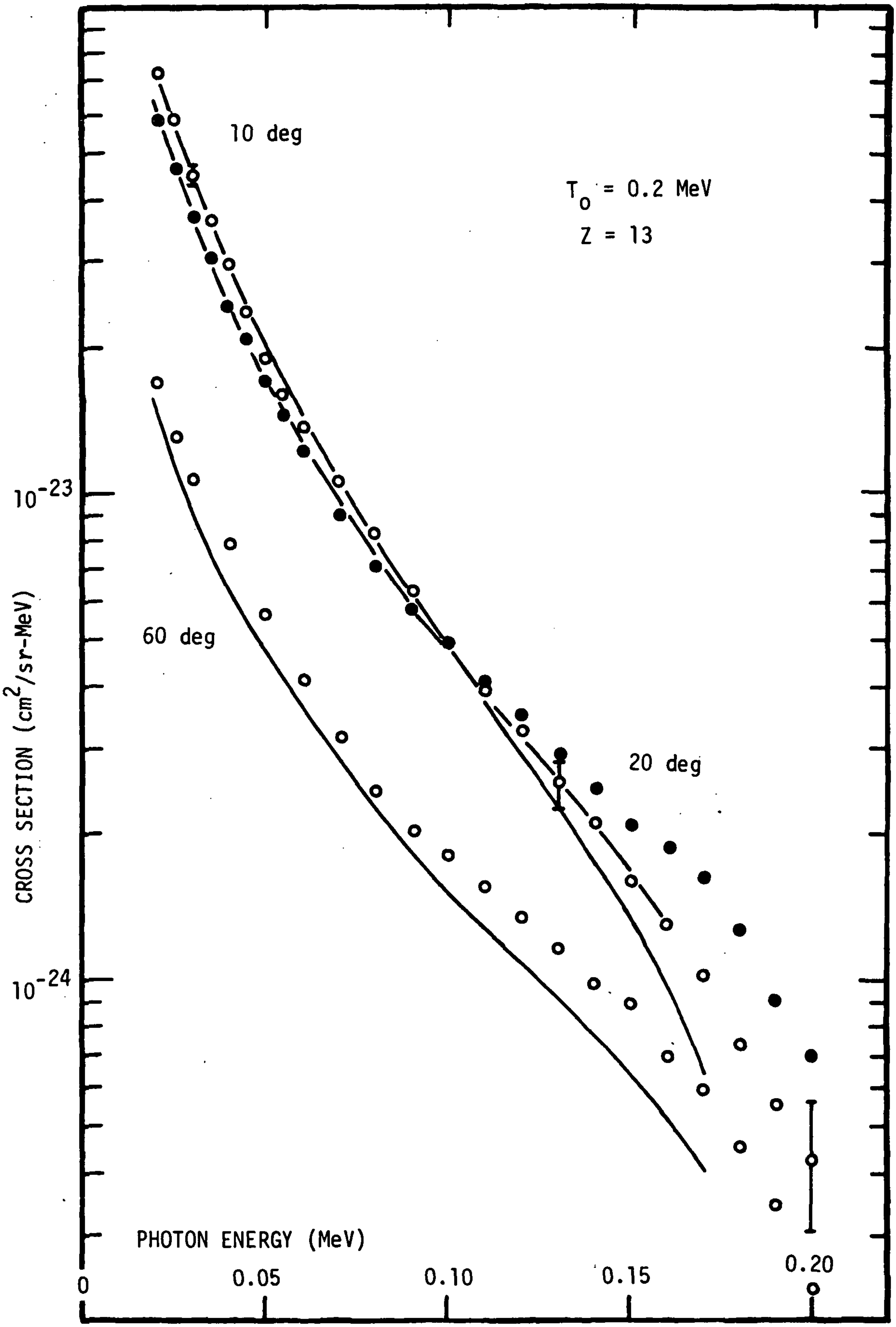

Fig. 6 Cross section spectra of bremsstrahlung from an Al target including the 20-deg spectrum.

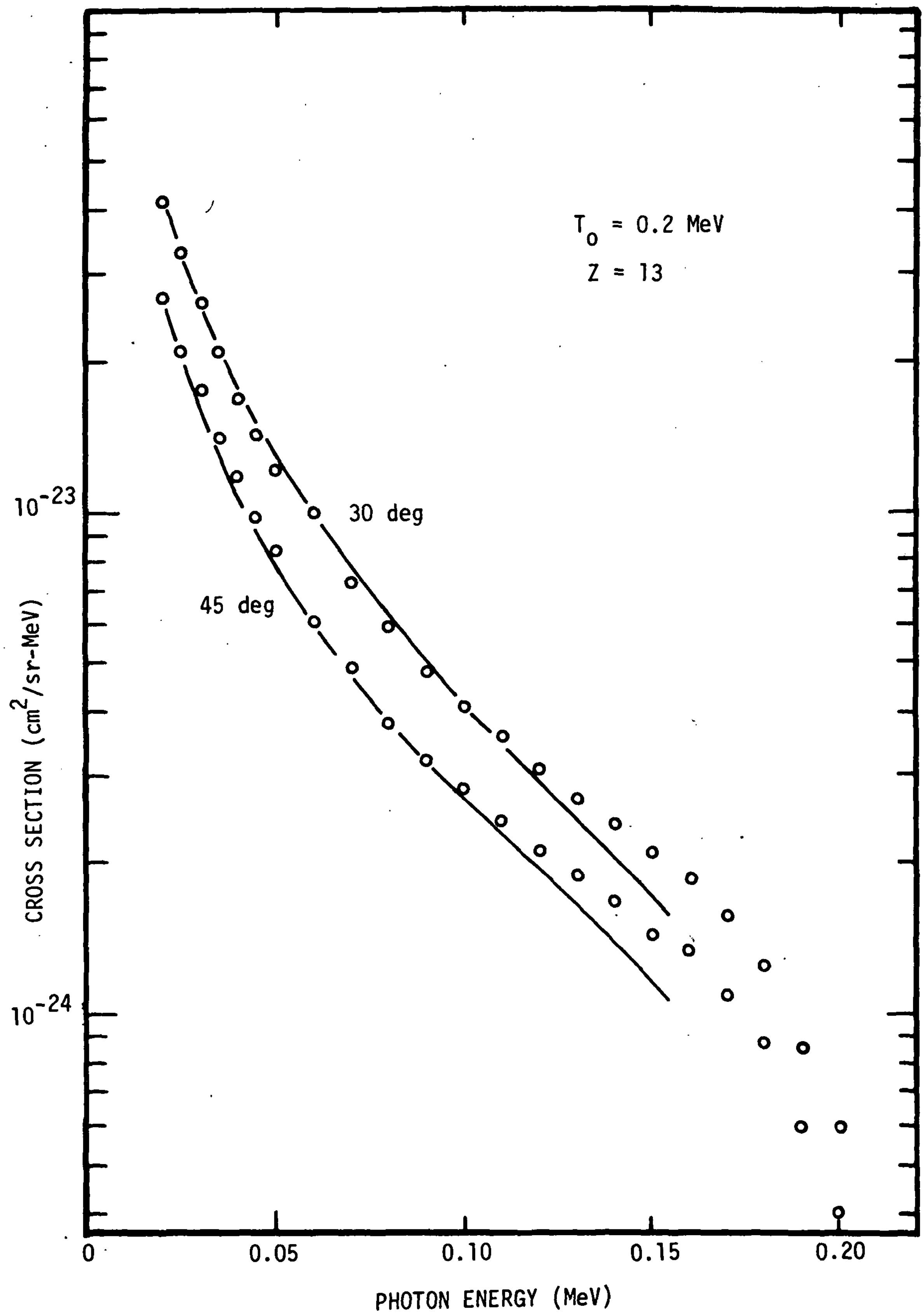

Fig. 7 Cross section spectra of bremsstrahlung for Al for photon emission angles of 30 and 45 deg.

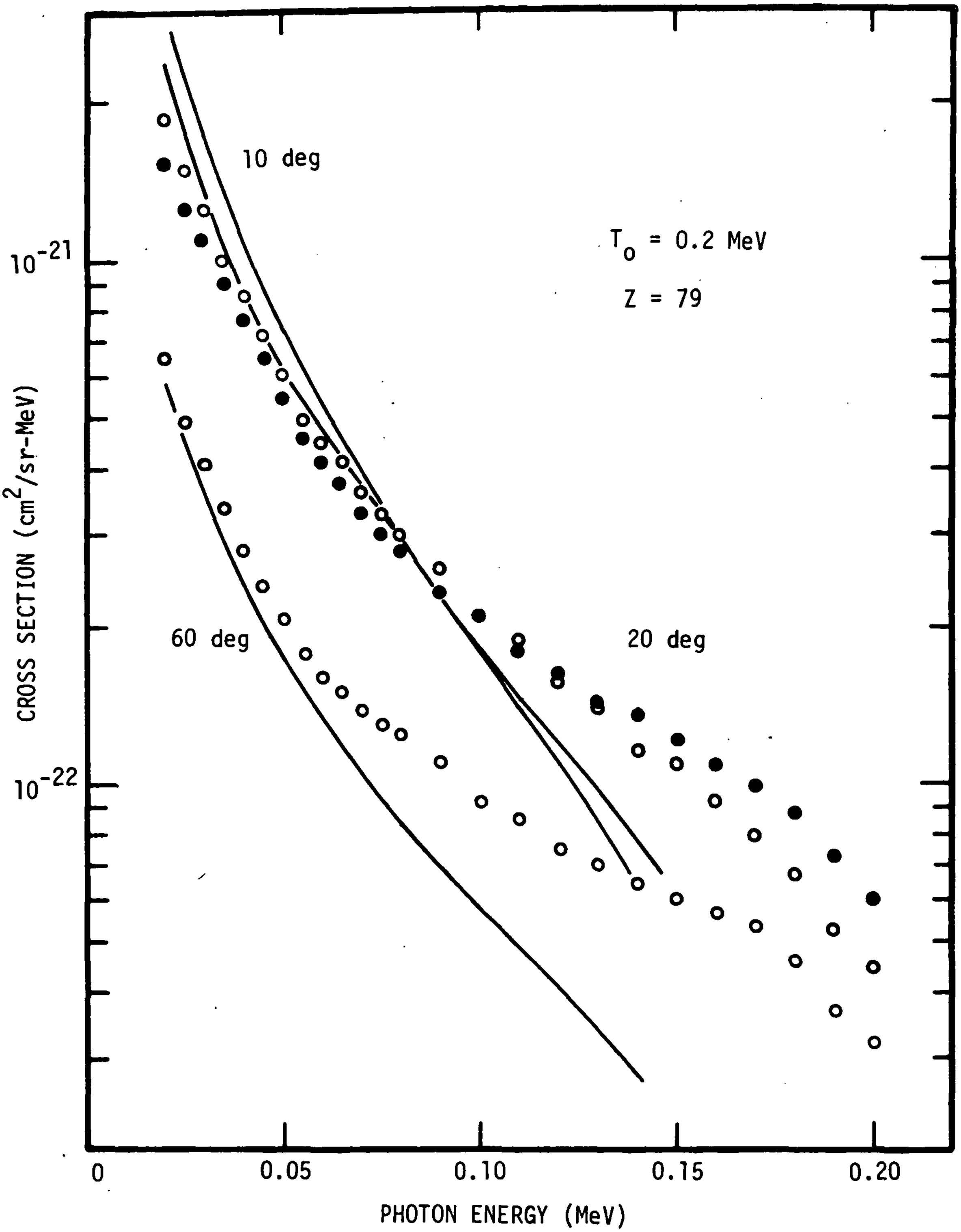

Fig. 8 Cross section spectra of bremsstrahlung from a Au target.

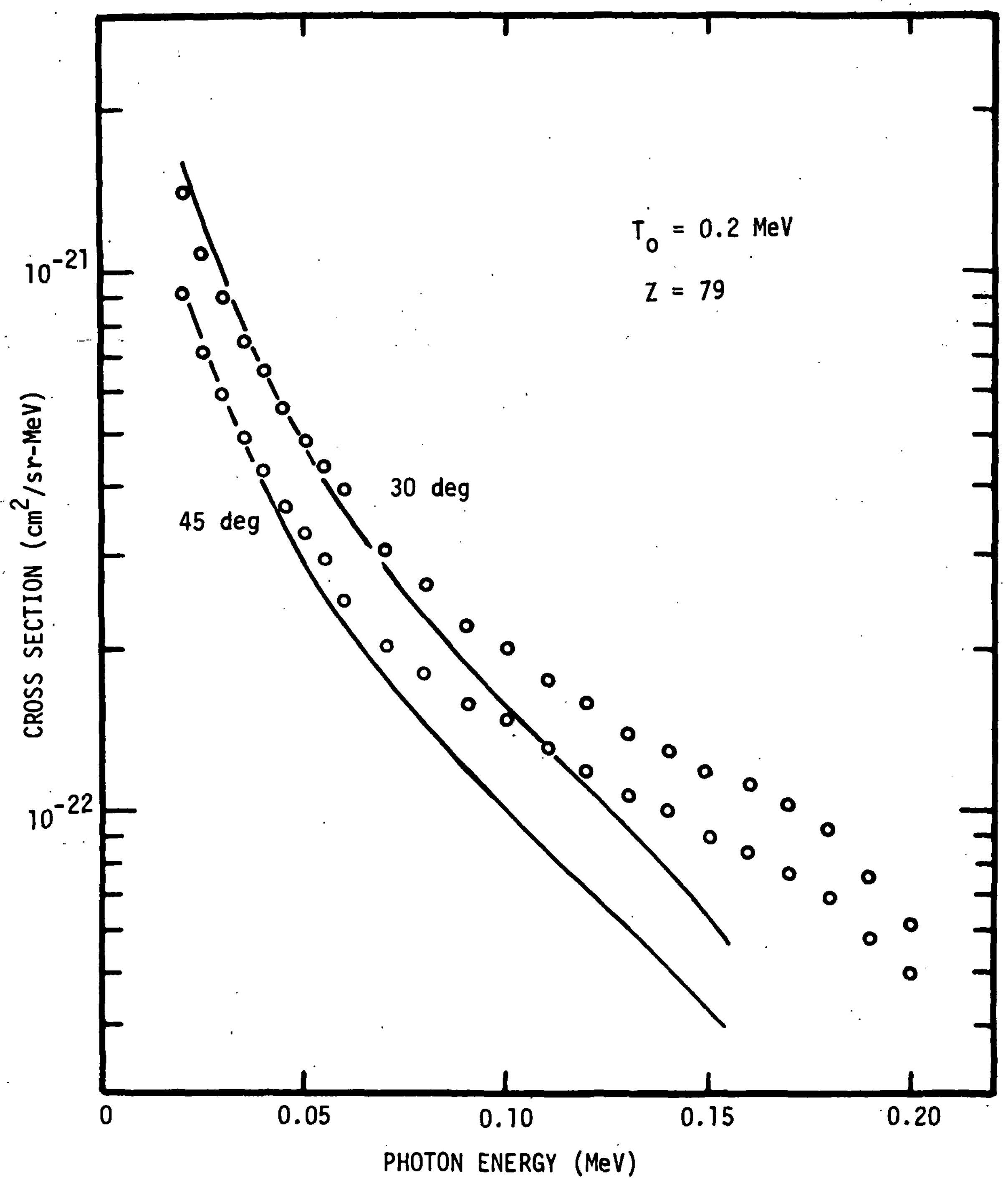

Fig. 9 Cross section spectra of bremsstrahlung for Au for photon emission angles of 30 and 45 deg.

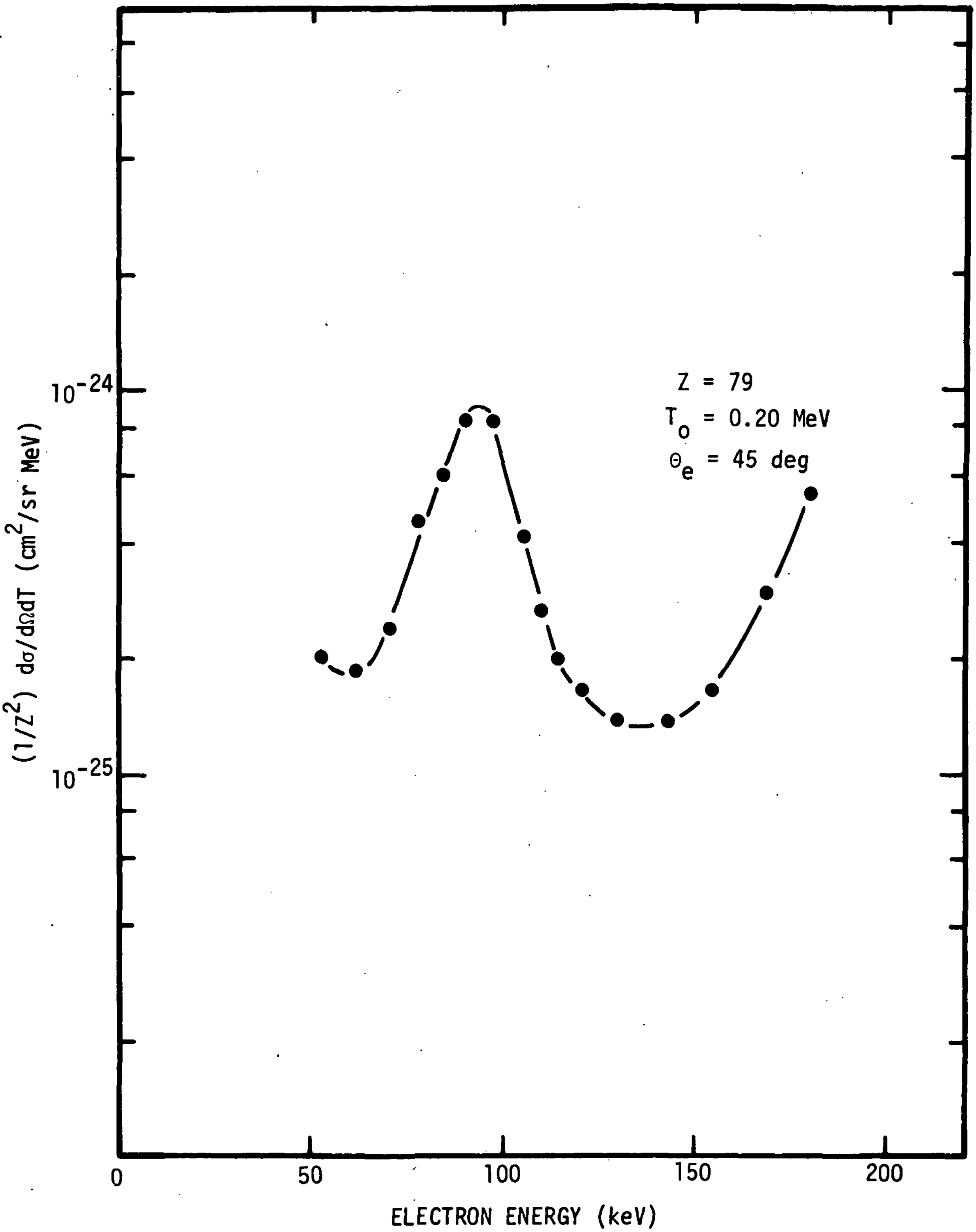

Fig. 10 Cross section spectrum of inelastically scattered electrons from a Au target. The plotted cross section values were computed from measurements by integrating over all photon angles.

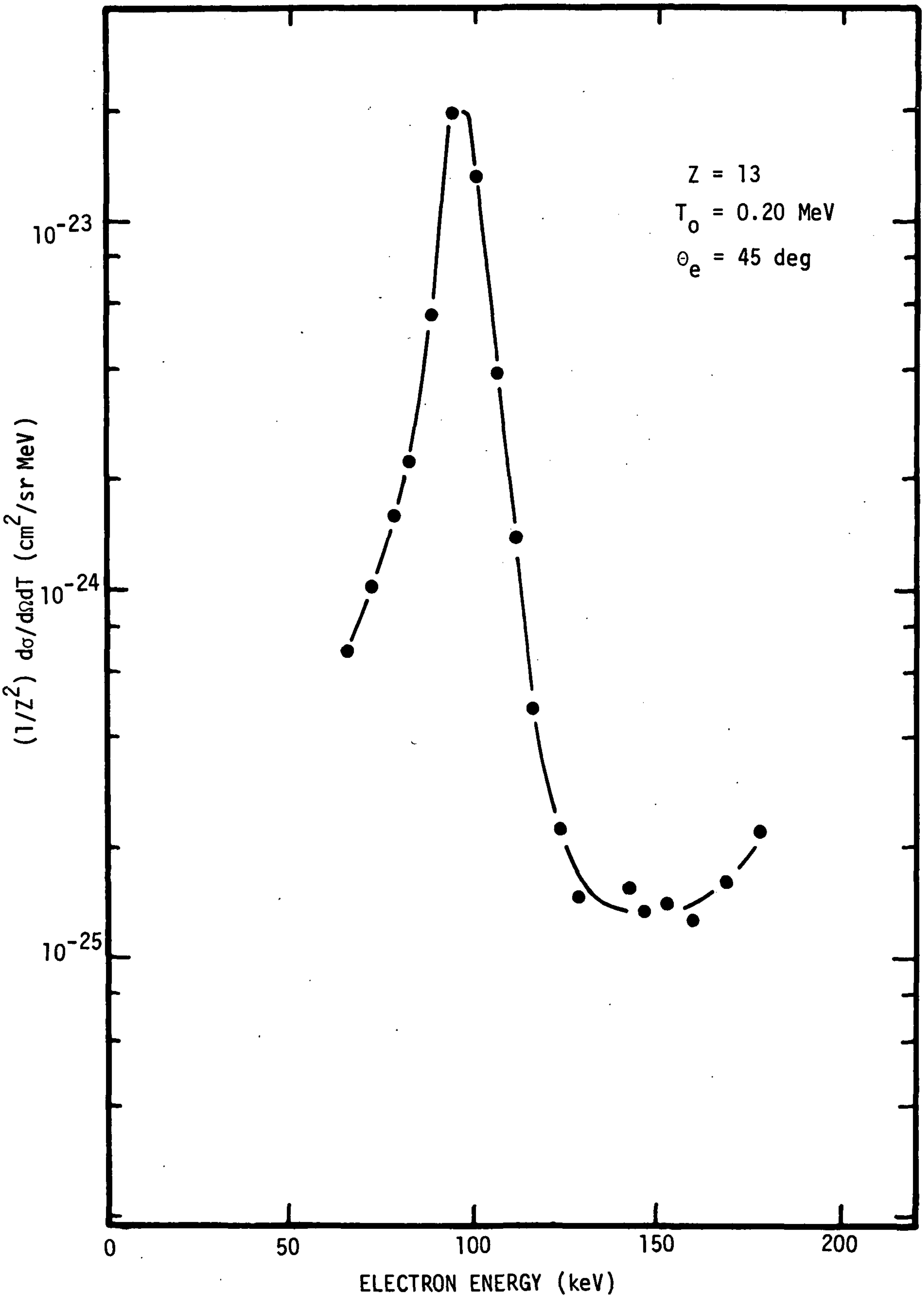

Fig. 11 Cross section spectrum of inelastically scattered electrons from an Al target. The electron-electron line is relatively intense for the low-Z target material.

less than 10% of the true rates. The dependency of the coincidence rates on the experimental parameters are defined by several simple expressions. The accidental coincidence rate is given by the expression

$$R_{AC} = 2\tau\ N_x\ N_e \tag{1}$$

where 2τ is the time-resolution of the coincidence circuit, N_x is the rate of x-ray detection, and N_e is the rate of electron detection. The rate of electron detection is further defined by the expression

$$N_e = (d\sigma/d\Omega dE)\ \Delta\Omega_e \Delta E\ N_a\ I/e \tag{2}$$

where $d\sigma/d\Omega$ is the measured cross section, $\Delta\Omega_e$ is the effective solid angle including the transmission factor of the magnetic analyzer, N_a is the number of target atoms per sq. cm., I is the incident electron beam current, and e is the electronic charge in appropriate units. A similar expression is valid for N_x. The average rate of true coincidence events is given by the expression

$$R_{TC} = (d\sigma/d\Omega_e\ d\Omega_x\ dE)\ \Delta\Omega_e\ \Delta\Omega_x\ \Delta E\ \frac{I}{e}\ N_a \tag{3}$$

where the quantity in parentheses is the double differential cross section and ΔE is the smaller of the two energy increments in the individual channels. From equations (1) and (2) it is seen that the accidental coincidence rate is proportional to the square of the incident beam current and the square of the target thickness, while from equation (3) it is seen that the true coincidence rate is only proportional to these quantities. Furthermore both rates depend directly on the solid angle factors of the two channels. Thus the true coincidence rate can be made significantly greater than the accidental rate by increasing the solid angle increments while reducing the beam current and/or target thickness. This was done for the present measurements. An accidental rate of less than 10% was achieved as shown in Appendix I.

The doubly differential cross sections for Al and Au are given in Table I and are plotted in Figs. 12-13. The Born-approximation values are shown in the figures and are also given in the table for comparison to the

TABLE I. DOUBLY DIFFERENTIAL CROSS SECTION

Target	Incident Energy (MeV)	Electron Energy (MeV)	Reduced Cross Section (mb) Experimental	Theoretical (B-H)
Al	0.20	0.15	10.2 ± 2.5	13.6
Al	0.20	0.16	11.1 ± 2.8	17.5
Au	0.20	0.15	6.5 ± 1.6	13.6
Au	0.20	0.16	8.3 ± 2.1	17.5
Au	0.15	0.12	18.6 ± 4.7	24.7

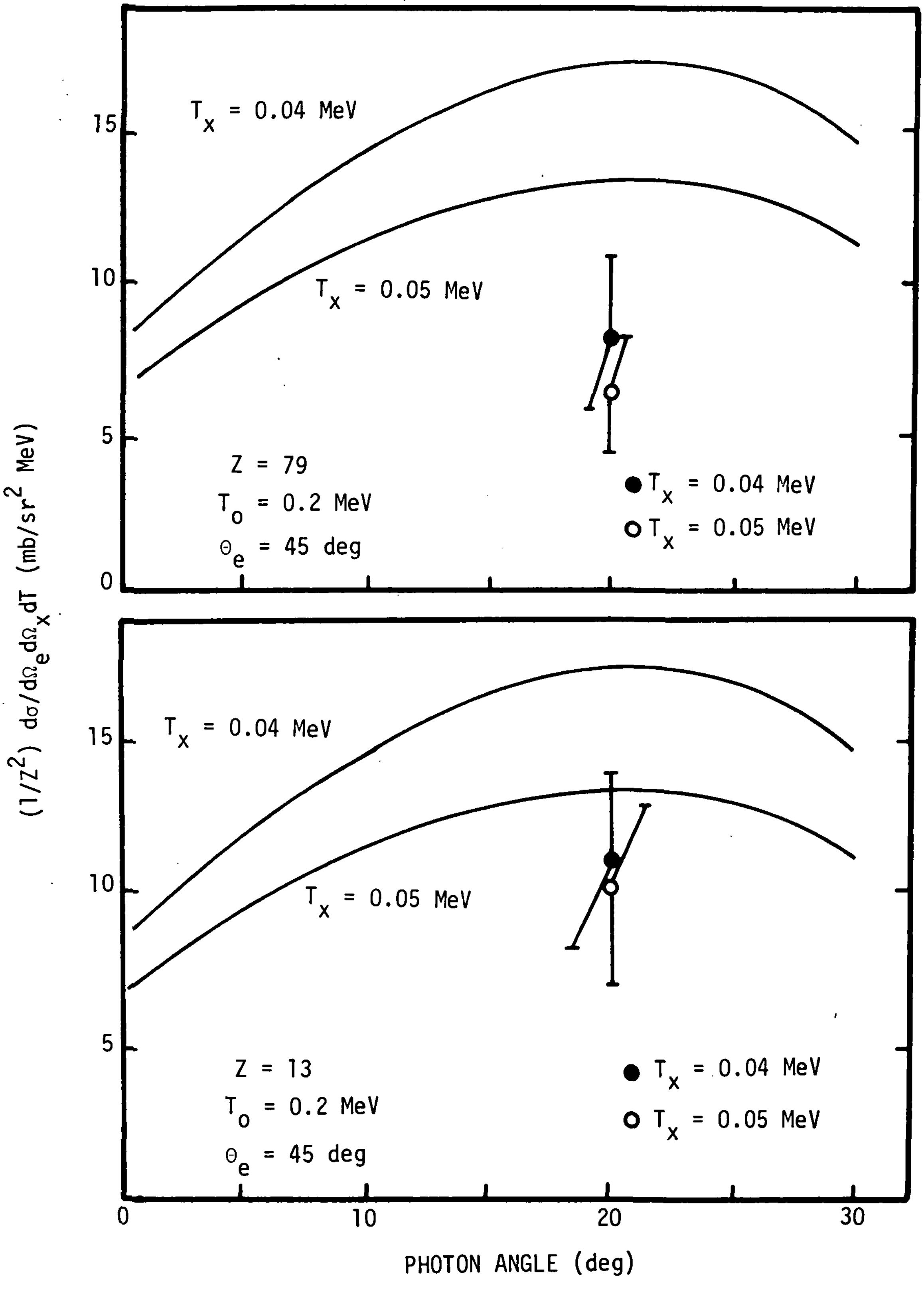

Fig. 12 Cross sections differential in photon angle, electron angle, and energy for Au (top) and Al for a bombarding energy of 0.2 MeV. Born-approximation values are shown for comparison.

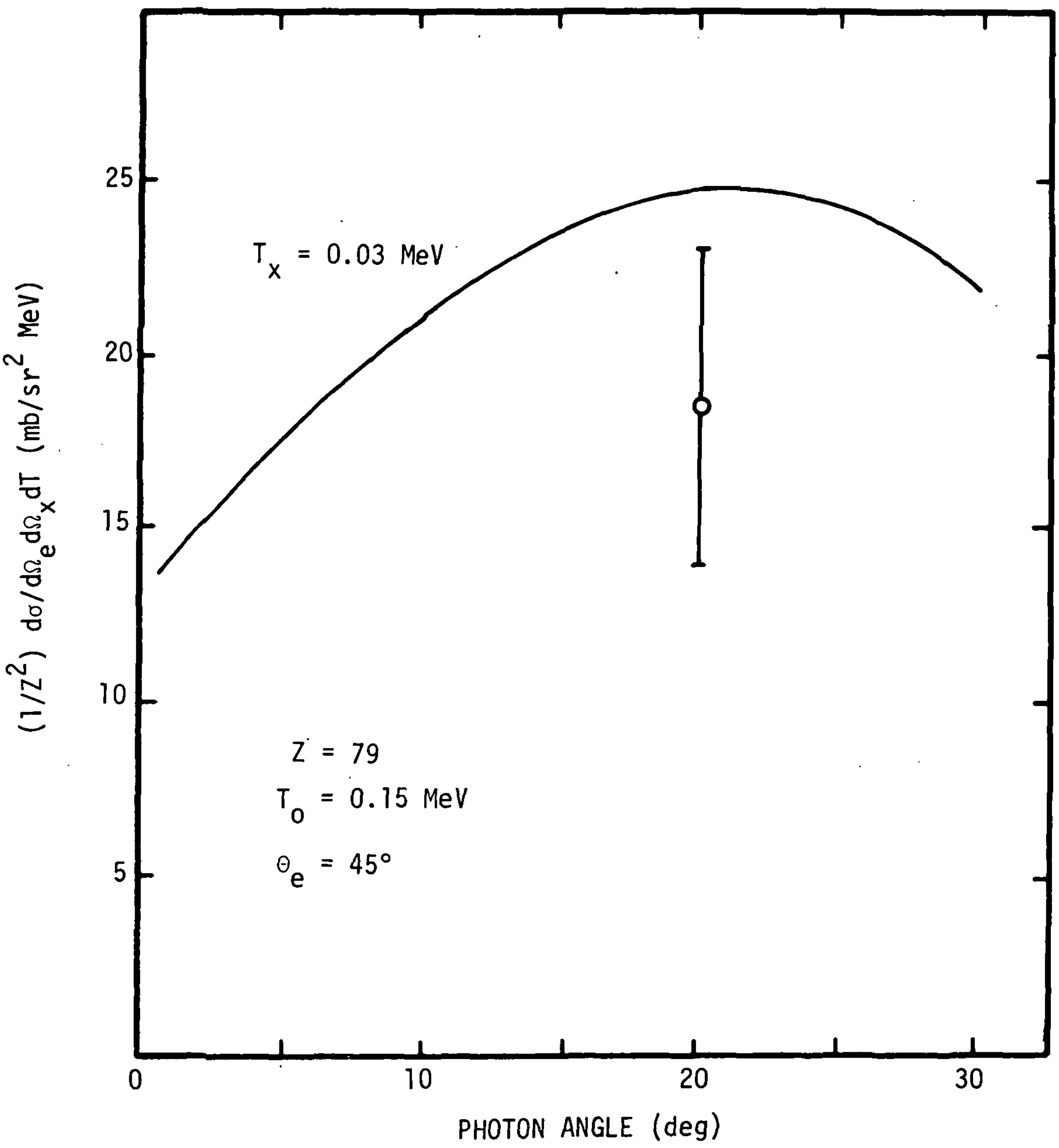

Fig. 13 Cross section differential in photon angle, electron angle, and energy for Au for a bombarding energy of 0.15 MeV. A photon energy increment of 10 keV centered at 30 keV was used.

measured values. In Fig. 12 the measurements for an inelastic energy of 0.16 MeV are plotted with solid circles and the measurements for 0.15 MeV, as open circles. An experimental error of 25% has been estimated for the experimental values. A total of one hundred coincidence counts were accumulated for each point, for which the statistical error is 10%. An uncertainty of about 5% is estimated for the target thickness determinations and about 7% for each of the solid angle factors. An uncertainty of 1-2% is estimated for the beam current measurements.

For Al the value of the cross section for an electron energy of 0.15 MeV, with the limits of error considered, is just below the Bethe-Heitler value, while the value for 0.16 is relatively lower. For Au at 0.2 MeV incident energy both values are significantly below the Bethe-Heitler values. The greater discrepancies in the case of the values for Au were expected, since the effect of screening for Au was found to be of the order of 30% in the singles measurement at 20 deg, as seen in Fig. 8. The Bethe-Heitler values, on the other hand, are for an unscreened point charge in both cases.

The measurement at 0.15 MeV bombarding energy was considered to be of importance, because as the incident energy is reduced, the angular distribution of events shifts to larger angles. Therefore the measurements at the electron angle of 45 deg at an incident energy of 0.15 MeV are more representative of the total number of events. The measurement was made for Au because of the relatively weaker electron-electron line for the high-Z target. Although the effect of screening complicates the comparison to the unscreened theory, the screening correction is about the same at this energy as at the higher energy. The measured value of the cross section is somewhat greater in comparison to the Bethe-Heitler values, but it is consistent with the comparisons at 0.2 MeV inasmuch as the singles yields in both channels are also relatively greater.

In conclusion, the measurements indicate that the electron-electron lines seen in the previously measured inelastic electron spectra influence the yield at higher energies. In addition, since the measured values of the doubly differential cross section are less than the values predicted by the Bethe-Heitler theory, the values at smaller angle must significantly exceed the approximate theory. It would be of interest to make an additional measurement

for a bombarding energy of 0.5 to 1.0 MeV with scintillation spectrometers so that a complete angular correlation curve with absolute yields could be obtained.

APPENDIX I

To establish the initial values of experimental parameters such as the electron and photon solid angle increments, the energy increment, and the incident electron beam current for the coincidence measurements, equations (1-3) were evaluated. Experimental cross section values were available which allowed accurate predictions of the expected detection rates in the separate channels. A somewhat higher detection rate was expected in the photon channel because of the inevitable presence of some background counts. To illustrate how these calculations were carried out and to confirm that the small contribution of the residual bremsstrahlung background which was totally uncorrelated with electron events did not affect the accuracy of the experiment, the following comparison of computed accidental and true concidence rates is included. The actual rates in the single channels, from which the spectra illustrated in Figs. 5 and 10 were obtained, have been used.

Typical values of the experimental parameters are given by the following equations:

$$\Delta E \Delta\Omega_e = 5.80(-6) \text{ sr MeV}, \tag{A-1}$$

$$\Delta E \Delta\Omega_x = 1.80(-5) \text{ sr MeV}, \tag{A-2}$$

$$I = 5.0(-9) \text{ A} \Rightarrow 3.12(10) \text{ e/sec}, \tag{A-3}$$

and

$$N_a = 1.53(17) \text{ atoms/cm}^2 \Rightarrow \bar{t} = 50\ \mu\text{g/cm}^2. \tag{A-4}$$

Values from Figs. 5 and 10 corresponding to cross section values for Z = 79 are

$$d\sigma/d\Omega dE_x = 6.5(-22) \text{ cm}^2/\text{sr MeV} \tag{A-5}$$

and

$$d\sigma/d\Omega dE_e = 8.10(-22) \text{ cm}^2/\text{sr MeV}. \tag{A-6}$$

If these quantities are combined according to Eq. (2), the detection rates in the individual channels are given by

$$N_x = 56 \text{ photons/sec} \tag{A-7}$$

and

$$N_e = 22 \text{ electrons/sec.} \tag{A-8}$$

The accidental coincidence rate R_{AC} given by Eq. (1) is computed to be, for a time resolution of 50 nanosec,

$$R_{AC} = 6.30(-5) \text{ coincidences/sec.} \tag{A-9}$$

On the other hand, by use of the doubly differential value measured for Z = 79 for a bombarding energy of 0.2 MeV and an inelastic energy of 0.15 MeV,

$$(1/Z^2)\ d\sigma/d\Omega_e d\Omega_x dE = 6.5(-27)\ \text{cm}^2/\text{sr}^2\ \text{MeV} \tag{A-10}$$

a true coincidence rate R_{TC} is computed by Eq. 3 to be

$$R_{TC} = 2.03(-3) \text{ coincidence/sec.} \tag{A-11}$$

The ratio of accidental to true rates is 0.03, or 3%. A similar analysis for a 70-μg/cm^2 Al target yields

$$R_{AC} = 1.02(-5) \tag{A-12}$$

and

$$R_{TC} = 8.20(-4). \tag{A-13}$$

The ratio of accidental rate to true rate is 0.012, or 1.2% for this case. In actual runs small changes in the solid angle increment of the photon channel were combined with variations in the beam current to maintain a desirable ratio

of accidental to true coincidences, while adjusting the absolute rates to practical values.

Since the doubly differential cross section value had not been obtained until the measurements were completed, the calculations were carried out with the value from the Bethe-Heitler theory.

REFERENCES

1. D. H. Rester and W. J. Rainwater, Phys. Rev. 138 (1965).
2. D. H. Rester and W. J. Rainwater, Phys. Rev. 140 (1965).
3. D. H. Rester and W. J. Rainwater, J. Appl. Phys. 37 (1966).
4. D. H. Rester and W. E. Dance, Phys. Rev. 161 (1967).
5. D. H. Rester, Nucl. Phys. A118 (1968).
6. D. H. Rester, N. Edmonson, and Q. Peasley, Phys. Rev. A 2 (1970).
7. D. H. Rester, W. E. Dance, and J. H. Derrickson, J. Appl. Phys. 41 (1970).
8. D. H. Rester and J. H. Derrickson, Nucl. Inst. Meth. 86 (1970).
9. D. H. Rester and J. H. Derrickson, J. Appl. Phys. 42 (1971).
10. D. H. Rester and N. Edmonson, Phys. Rev. A 4 (1971).
11. D. H. Rester and N. Edmonson, Phys. Rev. A 6 (1972).
12. H. Brysk, C. D. Zerby, and S. K. Penny, Phys. Rev. 180 (1969).

ADVANCED TECHNOLOGY CENTER, INC.

P.O. BOX 6144 DALLAS, TEXAS 75222